minerals

MDPI

Article

Trace Elements in Pernik Sub-Bituminous Coals and Their Combustion Products Derived from the Republika Thermal Power Station, Bulgaria

Mariana G. Yossifova [1,*], Greta M. Eskenazy [2], Stanislav V. Vassilev [3] and Dimitrina A. Dimitrova [1]

[1] Geological Institute, Bulgarian Academy of Sciences, "Acad. Georgi Bonchev" Str., Bl. 24, 1113 Sofia, Bulgaria; didi@geology.bas.bg
[2] Faculty of Geology and Geography, Sofia University "St. Kl. Ohridski", Tzar Osvoboditel Str. 15, 1504 Sofia, Bulgaria; greta@gea.uni-sofia.bg
[3] Institute of Mineralogy and Crystallography, Bulgarian Academy of Sciences, 1113 Sofia, Bulgaria; vassilev_stan@yahoo.com
* Correspondence: mariana@geology.bas.bg

Abstract: The contents of 49 trace elements in sub-bituminous Pernik coals and their waste products from preparation and combustion processes were investigated. The studied coals have trace element contents higher than the respective Clarke values for brown coals and some of them may pose environmental concerns. The elements Li, Rb, Cs, Ba, Sc, Y, La, Ce, Nd, Sm, Eu, Er, Ga, Zr, Sn, V, Nb, Ta, W, F, Cu, Zn, In, Pb, Cr, Co, Ni, and Th in the feed coals have concentrations that exceed twice the Clarke values. Most element contents in bottom ash are enriched compared with those in feed coal. Some of the volatile elements are equal or significantly depleted including Sn, Mo, Sb, F, Bi, Cd, Ge, and Pb. Fly ash has higher contents of Ga, Zr, Hf, Sn, V, Nb, Mo, and F in comparison with bottom ash. Most elements have a significant positive correlation with ash yield, indicating their inorganic association. The mixed wastes (coal slurry, bottom ash, and fly ash) in the disposal pond are slightly depleted of most of the elements studied with the exclusion of Cl, Ba, and Br. The Pernik coals and their waste products are unpromising for the extraction of REY due to their low element contents.

Keywords: trace elements; sub-bituminous coal; combustion wastes; Pernik TPS; Bulgaria

Citation: Yossifova, M.G.; Eskenazy, G.M.; Vassilev, S.V.; Dimitrova, D.A. Trace Elements in Pernik Sub-Bituminous Coals and Their Combustion Products Derived from the Republika Thermal Power Station, Bulgaria. *Minerals* **2024**, *14*, 313. https://doi.org/10.3390/min14030313

Academic Editors: Ivica Ristović and Shifeng Dai

Received: 17 November 2023
Revised: 4 March 2024
Accepted: 13 March 2024
Published: 16 March 2024

1. Introduction

In the processes of coal beneficiation and coal combustion in thermoelectric power stations (TPSs), several major waste products are generated, namely coal slurry, associated host rocks, bottom ash, and fly ash. It is well known that the detailed knowledge about the mineralogy and inorganic chemistry of these products has important fundamental, technological [1–9], and ecological [10–15] significance. Therefore, valuable information on the inorganic composition of coals and their combustion products has been summarized in several monographs [16–19].

Therefore, the scope of this investigation is to present additional data on the concentration, modes of occurrence, and behavior of 49 trace elements (Li, Rb, Cs, Sr, Ba, Tl, Be, Sc, Y, La, Ce, Pr, Nd, Sm, Eu, Gd, Tb, Dy, Ho, Er, Tm, Yb, Lu, Ga, Ge, Zr, Hf, Sn, V, Nb, Ta, Mo, W, F, Cl, Br, Cu, Zn, Cd, In, Pb, Bi, Sb, Cr, Mn, Co, Ni, Th, and U) in the Pernik coals and their beneficiation and waste products generated by the Pernik coal preparation plant (CPP) and Republika TPS. For the first time, the contents of the critical elements REY, Hf, Sc, Ta, and others, as well as the hazardous F are studied in the following samples: run-of-mine sub-bituminous coal, feed coal, high-grade coal, vitrain, coal slurry, associated host rocks, fly ash, bottom ash, and mixed material from the coal beneficiation and combustion processes, taken from the disposal pond. The potential environmental impacts related to hazardous elements in the aforementioned coals and products are further evaluated due to health concerns.

Data on the concentrations of fluorine in Bulgarian coal are scarce. Eskenazy and Dai [20] published such data for the first time, but they were mostly for coal of noneconomic importance. It should be noted that in 2023 the European Commission updated the list of critical elements by including As, He, Mn, Cu, and Ni, and removing In [21].

The first industrial coal mining in Bulgaria started in the Pernik coal basin in 1891 [22] and, as a result, the first Bulgarian TPS was built in the Pernik town during 1895. Presently, the mining of these Late Oligocene–Miocene sub-bituminous coals and their combustion in the Republika TPS are still active. The Pernik coal preparation plant (CPP) and 105 MV Republika TPS with three units are located in Pernik town (Figure 1) surrounded by three open-pit mines and numerous waste storage facilities related to coal utilization.

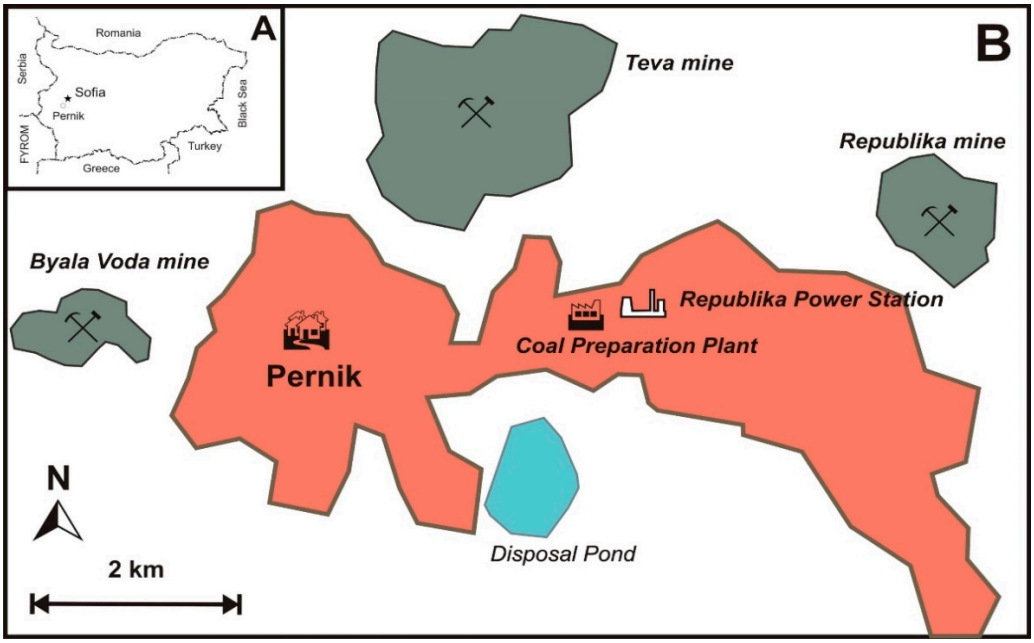

Figure 1. (**A**) Map of Bulgaria and (**B**) location of the Pernik coal preparation plant, the Republika thermoelectric power station, and the Pernik coal mines.

Data about the mineralogical and chemical characterization of the Pernik coals and the solid wastes from their beneficiation and combustion have been the subject of several investigations [23–28]. The common characteristics of this fuel are 47%–60% ash content, as-received basis (A_{ar}), 6%–14% moisture, as-received basis (W_{ar}), 21% volatile matter, as-received basis (VM_{ar}), 74% carbon, dry ash-free basis (C_{daf}), 16% oxygen, dry ash-free basis (O_{daf}), 5% hydrogen, as-received basis (H_{daf}), 3% nitrogen, dry ash-free basis (N_{daf}), 1% sulfur, dry ash-free basis (S_{daf}), and 2100–2200 kcal kg^{-1} calorific value, dry ash-free basis (Q_{daf}) [27]. The present work notes (1) the dominant role of inorganic matter as a source and concentrator of trace elements in Pernik coals; (2) the preservation of the intimate relationships of some authigenic minerals (pyrite, siderite, and clay minerals) with the organic matter [28] even after combustion process due to the formation of an oxide or aluminosilicate film on the surface of unburned organic particles; (3) the affinity of V, Mo, Ni, Pb, W, and HREEs to the organic matter; and (4) the migration of Ge, Mo, Br, F, and Bi with flue gases. For example, it was identified that the characteristic features of the sub-bituminous Pernik coal include very high ash yield; abundance of detrital quartz and feldspars and authigenic kaolinite, siderite, and pyrite; enrichment of Co, Cr, Cu, Ni, Pb, Rb, and Zn; affinity to organics and authigenic minerals of Br, Cl, Co, Ni, Pb, Sr, and Zn; detrital affinity of Li and Rb; and significant occurrence of water-soluble Cl and S [27]. The results also indicate some possible environmental pollution of the air (Br, Ce, Co, Cr, Eu, Hf, La, Mo, S, Sc, and Zn), water (Br, Cl, F, V, and Zn), soil (Ba, Co, Cu, Hf, La, Li, Mn,

Pb, and Sc), and vegetation (Ba, Bi, Cd, Pb, Sc, Sr, V, and Yb) in the areas surrounding the Republika TPS [27].

2. Coal Treatment and Burning

The Pernik coal preparation plant was built in 1953 for gravitational washing of the raw Pernik coals. In brief, the coals are manually separated, sieved, and briquetted. Feed coal (FC) for use in TPSs is obtained after coal sieving ($\leq$30 mm), but this fuel still has high ash yield (50%–60%). The high-grade coal (HGC) for home heating is generated by gravitational washing of the particles sized $\geq$30 mm. Finely ground magnetite and water from the Struma river are used as density media. The waste products from coal beneficiation are coal slurry (CS) and associated host rock (AR). These wastes are debris materials and commonly represent the non-coal-bearing strata. They consist primarily of materials from the partings of the coal beds, as well as materials from the mine roof and floor strata in the Pernik basin, which are incorporated into the coal during mining. A portion of epigenetic coarse-grained mineralization (mostly Fe-sulfides) in coals also occurs in these waste products after coal beneficiation. The coal-fired Republika TPS was built in 1951. Since then it has been supplied with sub-bituminous Pernik coals. The fly ash cleaning equipment of this pulverized coal-fired TPS with bottom ash discharged boilers includes mechanical collectors and three electrostatic precipitator rows [28].

3. Sampling and Methods

Eight types of solid composite samples of the Pernik sub-bituminous coals and their products generated by Pernik CPP and Republika TPS were collected and analyzed. Each composite sample included between 15–20 individual samples and weighed around 7–10 kg. They were taken from (1) a network of points at accessible locations in DP and from CPP warehouses; (2) the moving conveyor belts of the CPP at a certain time interval; and (3) the TPS director's average control samples used in the TPS laboratory in monitoring the quality of fuel and waste products. The samples include (1) run-of-mine sub-bituminous coal (RC); (2) feed coal (FC); (3) high-grade coal (HGC); (4) coal slurry (CS); (5) associated host rock (AR); (6) fly ash (FA); (7) bottom ash (BA); and (8) mixed material from the coal beneficiation and burning processes, which were taken from the disposal pond (DP). The samples were dried at room temperature and stored in plastic bags. The samples were repeatedly quartered and some of them were pre-crushed. Samples intended for chemical analyses and X-ray diffraction were powdered in an agate mortar. A vitrain (HGC) sample was manually separated and analyzed in order to distinguish the presence of organically associated trace elements. A split of the bottom ash sample was wet-screened in four size fractions (>1 mm, 1–0.5 mm, 0.5–0.25 mm, and <0.25 mm), which were analyzed for all elements except chlorine and bromine.

The ash yield of all samples was generated at 500 °C for 12 h in an open electric furnace as the temperature was gradually raised according to ISO 1171:2010 [29] for ash determination in solid mineral fuels. Inductively coupled plasma mass spectrometry (ICP-MS) in pulse counting mode was used to determine trace elements in the samples. For ICP-MS analysis, the samples were digested using a Milestone ultraCLAVE Microwave Digestion System with high-pressure reactor (Sorisole, Italy). The basic load for the digestion tank was composed of 330 mL of distilled water, 30 mL of 30% H_2O_2 (Metal–Oxide Semiconductor, MOS reagent), and 2 mL of 98% H_2SO_4 (Guaranteed reagent, GR). Initial nitrogen pressure was set at 50 bars and the highest temperature was set at 240 °C for 75 min. The reagent digestion for each 50 mg coal sample included 5 mL of 65% HNO_3 and 5 mL of 40% HF, but for non-coal samples, the reagents were 2 mL of 65% HNO_3 and 5 mL of 40% HF. Multi-element standards (Inorganic Ventures: CCS-1, CCS-4, CCS-5, and CCS-6) were used for the calibration of trace element concentrations [30]. Chlorine and bromine analyses were conducted by X-ray fluorescence method on pelletized coal samples [26]. Fluorine was determined by pyrohydrolysis in conjunction with a fluorine ion-selective electrode following the methods described in ASTM Standard D5987-96 [31].

Mineralogical investigations were performed by semiquantitative powder X-ray diffraction (XRD) using a diffractometer with Fe-filtered Co Kα and Ni-filtered Cu Kα radiations. Char particles present in fly ash were observed and selected using a binocular microscope. Their morphology and semi-quantitative chemical composition were studied using the following scanning electron microscope: SEM-EDS by means of Jeol Superprobe 733 (Jeol Ltd., Tokyo, Japan), at accelerating voltage of the probe 15 keV, and beam current 1 nA and 6×10^{-2} nA, for analyses and pictures, respectively. Prior to analyses, a thin carbon layer was sputter-coated on the samples.

4. Results

4.1. Mineralogy of the Coals and Combustion Products

The major minerals (>3 wt%, coal basis) in the coal samples are quartz, kaolinite, and pyrite. The minor minerals (1–3 wt%) are illite, plagioclase, K-feldspar, gypsum, calcite, dolomite, and siderite. The mineral composition of the coal slurry (CS) and associated rocks (ARs) is similar to that of coal; however, the contents of quartz, kaolinite, illite, K-feldspar, plagioclase, siderite, and calcite in CS and AR are higher than in coal [28].

Fly ash (FA) and bottom ash (BA) are represented by glass, quartz, mullite, K-feldspar, plagioclase, kaolinite, magnetite, hematite, and traces of calcite, gypsum, lime, maghemite, illite, Ca_2SiO_4, and char (Figure 2). The common minerals for all FA and BA samples are quartz and kaolinite.

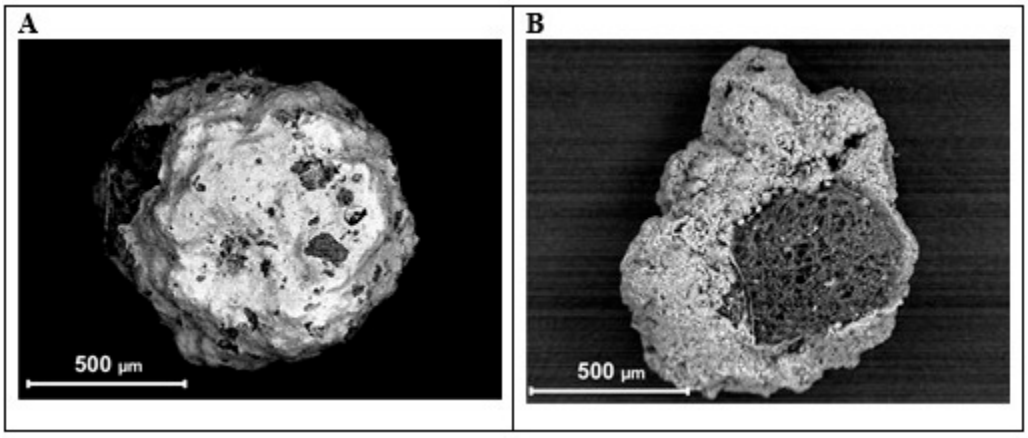

Figure 2. SEM back-scattered images of (**A**) porous spheroidal char covered with Fe oxide film (fly ash, fraction 1–0.5 mm); (**B**) fusinoid char covered with aluminosilicate film (fly ash, fraction 1–0.5 mm).

4.2. Trace Elements

The samples were analyzed for 49 trace elements and the concentrations of these elements in the coals were compared with the Clarke contents (worldwide averaged values) for brown coals [1] (Tables 1–3). A concentration coefficient (CC) [32] is introduced herein, which expresses the ratio between the element content in coal to the relevant Clarke value. According to this coefficient, the concentrations of trace elements in coal samples can be presented in the following decreasing order: FC > RC > HGC > vitrain. The element contents in bottom ash were compared with those in feed coal. In order to evaluate the element redistribution, the enrichment coefficients FA/BA were calculated. The behavior of the REEs in all studied samples was coherent and the europium anomaly was very weak (Eu/Eu* = 0.69–0.79) (normalized to chondrite) [33]. Most elements showed a high positive correlation ($r > 0.90$) with ash yield, indicating their inorganic association. The wastes from the disposal pond were characterized by increased contents of Cl, Ba, and Br.

Table 1. Element contents (ppm) in coals, coal slurry, associated rocks, and mixed material from DP.

Elements	Samples							World [a] Averages
	RC	HGC	FC	CS	DP	AR	Vitrain	
				Lithophile elements				
Li	46	18	46	43	69	51	6.0	10
Rb	73	27	77	69	88	91	6.5	10
Cs	12	2.7	7.3	6.9	9.8	7.6	0.7	0.98
Sr	245	90	195	158	199	224	84	120
Ba	304	130	315	546	410	376	105	150
Tl	0.57	0.2	0.65	0.66	0.82	0.63	0.02	0.68
Be	2.42	2.3	2.11	2.2	3.2	2.13	1.3	1.2
Sc	16	8.6	15	13.9	21	17	4.5	4.1
Y	20	14	18	17.6	27	22	7.4	8.6
La	27	12	24	22	34	29	4.2	10
Ce	55	24	48	44	74	58	8.9	22
Pr	6.3	2.8	5.6	5.2	8.2	6.7	0.98	3.5
Nd	29	12	23	21	33	28	4.5	11
Sm	5.1	2.5	4.6	4.2	6.8	5.5	0.93	1.9
Eu	1.2	0.64	1.12	1.11	1.7	1.34	0.27	0.50
Gd	5.4	2.8	4.8	4.5	7.1	5.8	1.11	2.6
Tb	0.71	0.4	0.64	0.59	0.95	0.77	0.18	0.32
Dy	4.0	2.5	3.7	3.47	5.4	4.4	1.26	2.1
Ho	0.74	0.49	0.68	0.64	1	0.81	0.26	0.50
Er	2.21	1.54	2.10	1.97	3.1	2.4	0.86	0.85
Tm	0.3	0.21	0.30	0.26	0.41	0.32	0.11	0.31
Yb	2.1	1.53	1.93	1.89	2.9	2.27	0.84	1.0
Lu	0.29	0.22	0.27	0.27	0.41	0.32	0.12	0.19
Ga	20	9.1	19.1	17.3	27	21	5.5	5.5
Ge	1.4	0.84	1.56	1.45	1.4	1.22	1.25	2.0
Zr	77	36	74	68	116	87	30	35
Hf	2.14	0.96	2.15	1.9	3.2	2.42	0.8	1.2
Sn	2.28	0.85	2.23	1.96	2.75	2.55	0.41	0.79
V	165	111	173	153	227	142	140	22
Nb	7.5	3.6	7.7	6.9	11	8.5	4.6	3.3
Ta	0.58	0.19	0.56	0.46	0.78	0.64	0.12	0.26
Mo	2.4	4.6	2.9	3	2.82	1.61	5.5	2.2
W	2.74	2.4	2.81	2.61	4.26	2.59	5	1.2
F	500	207	446	420	415	543	104	90
Cl	48	78	21	80	90	47	nd	120
Br	7.1	8.3	5.8	7.3	5	6.7	nd	4.4

Table 1. *Cont.*

Elements	Samples							World [a] Averages
	RC	HGC	FC	CS	DP	AR	Vitrain	
Sulfophile elements								
Cu	91	38	80	70	117	85	16	15
Zn	68	35	63	69	95	88	8.8	18
Cd	0.43	0.33	0.32	0.36	0.34	0.46	0.14	0.24
In	0.07	0.03	0.07	0.06	0.09	0.078	0.01	0.021
Pb	29	19	28	30	28	45	12	6.6
Bi	0.59	0.24	0.52	0.38	0.41	0.57	0.1	0.84
Sb	0.84	0.7	0.96	0.85	1.0	0.98	0.86	0.84
Siderophile elements								
Cr	49	24	50	44	81	58	15	15
Mn	65	122	86	223	245	433	57	71
Co	12	9.9	12	12	20	16	5.5	4.2
Ni	32	21	28	30	49	33	17	9.0
Radioactive elements								
Th	15	6.1	13	12.3	19	15	2.8	3.3
U	7.1	3.1	5.9	5.8	8.8	5.7	2.2	2.9
Ash yield, %	59.2	26.8	59.9	70.4	95.6	79.1	8.8	

[a]—World average values for brown coals by Ketris and Yudovich [1]. nd—not determined.

Table 2. Trace element contents in bottom ash and respective size fractions, ppm.

Elements	BA	BA >1 mm	BA 1–0.5 mm	BA 0.5–0.25 mm	BA <0.25 mm	e/d	BA/FC
Fraction Yield, %		**3.1**	**13.6**	**41.6**	**41.7**		
Lithophile elements							
Li	69	46	62	71	71	1.54	1.50
Rb	118	76	110	125	109	1.43	1.53
Cs	9.5	6.0	8.5	9.8	9.6	1.60	1.30
Sr	261	167	248	265	257	1.54	1.34
Ba	721	309	634	693	717	2.32	2.28
Tl	0.79	0.76	0.82	0.80	0.75	0.98	1.22
Be	2.8	2.5	2.5	2.8	2.8	1.12	1.33
Sc	22	16	20	23	23	1.43	1.47
Y	27	23	25	27	28	1.22	1.50
La	36	23	32	36	36	1.56	1.50
Ce	74	48	67	75	75	1.56	1.54
Pr	8.5	5.6	7.7	8.6	8.7	1.55	1.51
Nd	35	23	32	35	35	1.52	1.52
Sm	6.8	4.7	6.4	6.9	7.1	1.51	1.45
Eu	1.74	1.17	1.60	1.75	1.78	1.52	1.55

Table 2. *Cont.*

Elements	BA	BA >1 mm	BA 1–0.5 mm	BA 0.5–0.25 mm	BA <0.25 mm	e/d	BA/FC
Fraction Yield, %		**3.1**	**13.6**	**41.6**	**41.7**		
Gd	7.17	5.08	6.78	7.25	7.41	1.46	1.49
Tb	0.94	0.71	0.90	0.95	0.97	1.37	1.47
Dy	5.47	4.34	5.18	5.50	5.70	1.31	1.48
Ho	1.01	0.82	0.95	1.02	1.04	1.27	1.48
Er	3.05	2.55	2.87	3.06	3.15	1.23	1.45
Tm	0.40	0.34	0.38	0.40	0.42	1.23	1.33
Yb	2.90	2.39	2.74	2.94	3.04	1.27	1.50
Lu	0.41	0.34	0.39	0.41	0.42	1.23	1.52
Ga	24	18	23	25	24	1.33	1.25
Ge	1.3	1.85	1.52	1.20	1.20	0.65	0.83
Zr	112	90	107	111	112	1.24	1.51
Hf	3.16	2.45	2.92	3.02	3.03	1.23	1.47
Sn	2.25	2.10	3.39	2.19	2.16	1.03	1.00
V	213	228	207	211	220	0.96	1.23
Nb	10.7	8.3	9.9	10.8	10.9	1.31	1.38
Ta	0.83	0.58	0.76	0.83	0.81	1.40	1.48
Mo	3.0	4.2	4.4	2.90	3.10	0.74	1.03
W	3.5	2.9	3.8	3.40	3.40	1.17	1.24
F	301	317	408	318	242	0.76	0.67
Cl	55	nd	nd	nd	nd		
Br	2	nd	nd	nd	nd		
Sulfophile elements							
Cu	111	88	120	111	120	1.36	1.38
Zn	81	65	106	85	111	1.71	1.28
Cd	0.23	0.29	0.28	0.23	0.22	0.76	0.72
In	0.08	0.06	0.08	0.07	0.07	1.16	1.14
Pb	26	26	31	25	24	0.93	0.92
Bi	0.16	0.27	0.25	0.13	0.20	1.31	0.31
Sb	0.96	1.48	1.56	0.88	0.89	1.20	1.00
Siderophile elements							
Cr	92	63	114	94	91	1.44	1.84
Mn	353	412	445	328	384	0.93	5.69
Co	23	19	23	23	25	1.31	1.91
Ni	59	55	71	61	66	1.20	2.11
Radioactive elements							
Th	18	12	16	19	19	1.58	1.46
U	7.2	6.1	6.4	7.0	7.5	1.23	1.22
Ash yield, %	94.3	64.3	88.6	96.2	97.7	1.51	1.57

e/d—enrichment/depletion coefficient; element contents in fraction <0.25 mm/element contents in fraction >1.0 mm; and BA/FC—element contents in bottom ash/element contents in feed coals.

Table 3. Trace element contents (ppm) in fly ash generated from the Republika power station.

Elements	Samples			m/b	e1/b	e2/b
	Mechanical Collector (MC)	Electrostatic Precipitators				
		1st Row (EP1)	2nd Row (EP2)			
			Lithophile elements			
Li	73	74	75	1.05	1.07	1.08
Rb	123	130	104	1.04	1.10	0.88
Cs	11.0	10	9.7	1.15	1.05	1.02
Sr	286	299	276	1.09	1.14	1.05
Ba	528	697	571	0.73	0.97	0.79
Tl	0.72	0.87	1.2	0.91	1.10	1.52
Be	2.9	3.01	3.44	1.03	1.07	1.23
Sc	24	25	24	1.09	1.13	1.09
Y	29	29	29	1.07	1.01	1.01
La	39	37	36	1.08	1.02	1.00
Ce	80	79	77	1.08	1.07	1.04
Pr	9.2	9.0	8.8	1.08	1.05	1.03
Nd	37	37	36	1.06	1.06	1.03
Sm	7.4	7.4	7.3	1.09	1.09	1.07
Eu	1.8	1.8	1.8	1.03	1.03	1.03
Gd	7.8	7.7	7.6	1.08	1.07	1.06
Tb	1.01	1.02	1.02	1.07	1.08	1.08
Dy	5.86	5.95	6.03	1.07	1.08	1.10
Ho	1.07	1.08	1.09	1.06	1.07	1.08
Er	3.27	3.29	3.36	1.06	1.08	1.10
Tm	0.44	0.43	0.44	1.10	1.07	1.10
Yb	3.1	3.2	3.2	1.07	1.10	1.10
Lu	0.44	0.44	0.45	1.07	1.07	1.10
Ga	24	28	36	1.00	1.16	1.50
Ge	1.17	2.4	4.2	0.90	1.84	3.23
Zr	110	130	142	0.98	1.16	1.27
Hf	3.12	3.6	3.9	0.98	1.14	1.23
Sn	2.30	3.2	4.8	1.02	1.42	2.13
V	213	280	328	1.00	1.31	1.54
Nb	10.9	12.4	13.8	1.02	1.16	1.29
Ta	0.91	0.95	0.99	1.09	1.14	1.19
Mo	2.77	3.8	5.7	0.92	1.26	1.90
W	3.9	3.4	4.4	1.11	0.97	1.26
F	303	571	1017	1.00	1.89	3.38
Cl	70	30	40	1.27	0.54	0.72
Br	3	5	2	1.5	2.50	1.00

Table 3. *Cont.*

Elements	Samples			m/b	e1/b	e2/b
	Mechanical Collector (MC)	Electrostatic Precipitators				
		1st Row (EP1)	2nd Row (EP2)			
			Sulfophile elements			
Cu	117	122	128	1.05	1.10	1.15
Zn	66	110	160	0.81	1.36	1.97
Cd	0.22	0.35	0.52	0.96	1.52	2.26
In	0.07	0.1	0.16	0.87	1.25	2.00
Pb	22	38	64	0.84	1.46	2.46
Bi	0.17	0.61	1.19	1.06	3.81	7.43
Sb	0.91	1.37	2.11	0.95	1.43	2.19
			Siderophile elements			
Cr	84	101	101	0.91	1.09	1.09
Mn	382	246	227	1.08	0.69	0.64
Co	21	22	22	0.91	0.96	0.96
Ni	48	61	62	0.81	1.03	1.05
			Radioactive elements			
Th	21	19	19	1.11	1.00	1.00
U	8.3	7.9	8.7	1.15	1.10	1.2
Ash yield.%	97.9	98.7	98.6	1.03		

m/b, e1/b, e2/b = (element contents in mechanical collector, 1st and 2nd EPS rows/element contents in bottom ash).

5. Discussion

5.1. Mineralogy of Combustion Products

The mineral composition of coals and associated rocks predetermines the mineralogy in the wastes from coal beneficiation and coal burning processes [34–38]. For example, the mullite content in fly ash from the Jungar Power Plant, Inner Mongolia, China, is as high as 37.4% because of high boehmite and kaolinite contents in feed coal [34]. The origin of the minerals and phases in FA and BA is discussed by a number of authors [24,34,39,40]. According to Vassilev [39], the primary minerals and phases are components originally present in coals that have not undergone phase transformations during the combustion process. The secondary phases form during burning, while the tertiary minerals originate during the transportation and storage of BA and FA.

The origin of newly formed phases/minerals in our study is (1) secondary for glass, mullite, hematite, lime, maghemite, Ca_2SiO_4, quartz, K-feldspar, plagioclase, kaolinite, illite, and magnetite; and (2) tertiary for calcite and gypsum. Incomplete coal combustion leads to excessive unburned carbon or char [41]. Organic–petrographic constituents in char are controlled by coal micro-lithotypes [41,42].

The main lithotypes in the studied coal samples are clarain and vitrain. The micro-lithotypes are mostly clarite, vitrite, and vitrinertite. Of the three maceral groups, vitrinite dominates [28]. The unburned carbon in the fly ash from the Republika TPS is about 2% as could be presumed by the loss of ignition (LOI) values. The studied char particles are elongated porous spheroids composed of altered vitrain and clarain. Some of the particles are covered with iron oxide formed as a result of the oxidation of pyrite or siderite (Figure 2A) or aluminosilicate (Figure 2B) film. The aluminosilicate film is most probably a phase of the transformation of clay minerals because traces of Mg, Ca, Ti, Al, Si, Fe, S, and Cu were identified in this film and char matrix. Most of these elements are present in

the clay minerals of Pernik coal [28]. Nano-particles of Fe, Cu, and Zn included in the char matrix were observed as well. According to Hower et al. [43], vitrinite is one of the main sources for the formation of char particles in the FA from low-rank coal combustion, but without it being melted and repolymerized. On the other hand, the constant heating of Pernik coals by active fires at depth, caused by their spontaneous combustion, is probably also a factor in the type of char particles formed [22,28,44]. During this process, volatile components are released [14], as well as a change in the vitrinite structure depending on the temperature and lack of oxygen [45,46].

5.2. Trace Elements

The mobility of trace elements during beneficiation and combustion depends on their mode of occurrence and concentrations in coal, as well as on the preparation and combustion technologies [35,47–49].

5.2.1. Trace Elements in Coals and Wastes from Preparation and Disposal Pond

The Pernik sub-bituminous coals supplying the Republika TPS have a high ash yield (Table 1). As a rule, the element contents and ash yields of the raw and feed coals are similar because the initial processing of raw to feed coal is crushing and sieving. When compared with the respective world averages for brown coals [1], the elements in the raw and feed coals are more or less enriched, excluding Tl, Ge, Bi, and Sb having similar or lower contents (Table 1, Figure 3). These observations indicate the leading role of inorganic matter as a contributor and concentrator of trace elements in Pernik coals.

The high-grade coals are depleted in all elements in comparison with the feed coals (Table 1). However, compared with the element contents of the world brown coals, the HGCs are enriched in some hazardous elements such as V > Pb > Cu > Co > Ni; F > Mo > Be; Zn > Br; and Th > Cr > Cd (Figure 3).

Vitrain is the most abundant lithotype in the HGCs. The sample studied (8.8% ash yield) has the lowest trace element contents compared with the feed coal and global averages. The only strongly enriched element is V and, to a lesser extent, Mo, Ni, Pb, and W (Table 1, Figure 3). The following factors can be supposed as a source of vanadium in the coal basin: (1) the Upper Cretaceous mafic and intermediate igneous rocks, which are in contact with the eastern and north-eastern margins of the Pernik basin; their V contents are up to 535 ppm and 320 ppm, respectively [50,51], and (2) the alternated host rocks of the Breznik and Klisoura polymetallic ore deposits, where the V contents are up to 320 ppm and 200 ppm, respectively [52,53]. Both deposits are located on the northern margin of the coal basin.

The associated host rocks have enhanced contents of all elements towards the Clarke concentrations, excluding Mo, Cl, and Br.

The above data show again the dominant inorganic affinity of most trace elements in the Pernik coals, which is one of the most significant factors for their behavior during combustion.

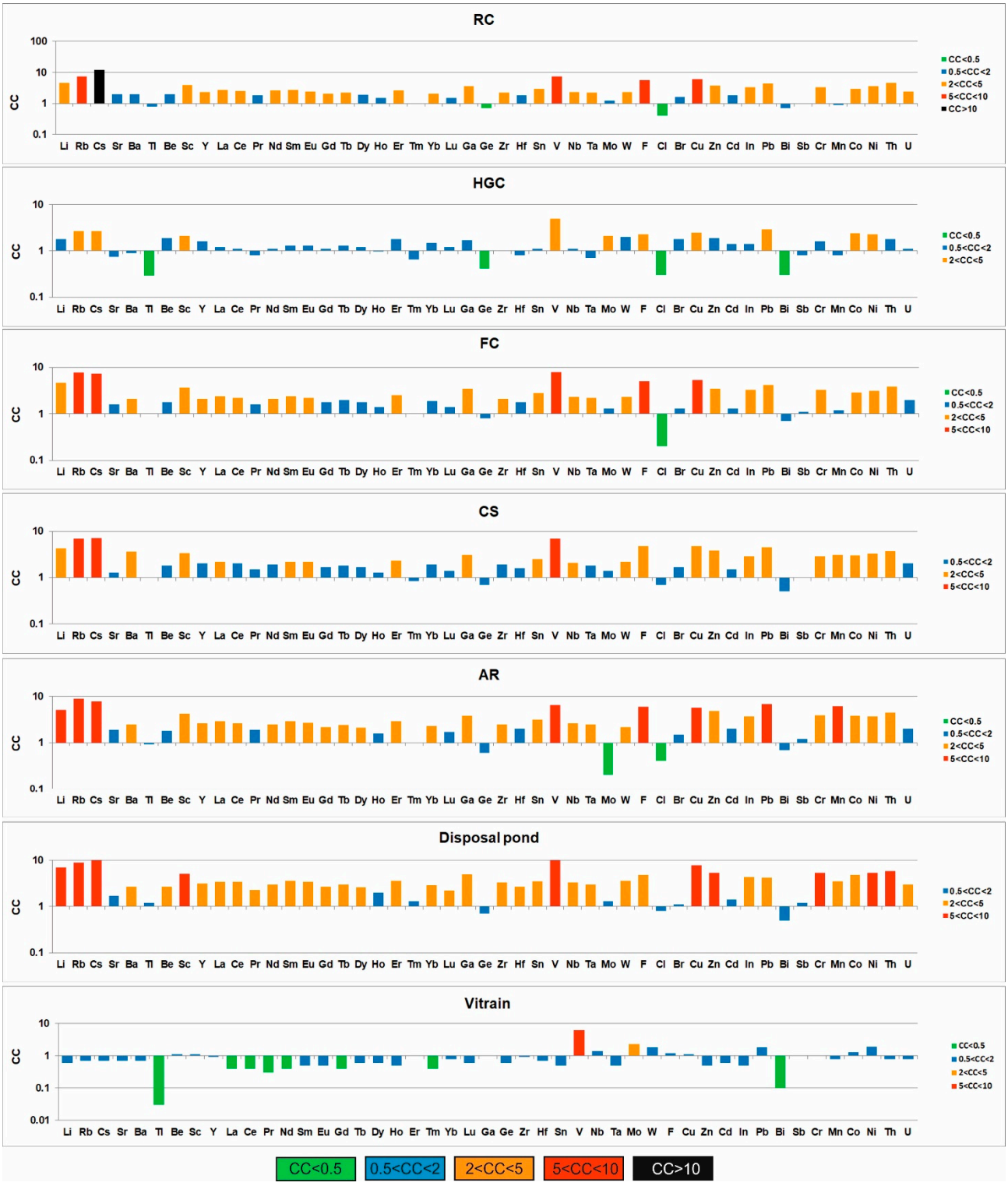

Figure 3. Concentration coefficients (CCs) [32]: trace element contents in the Pernik coals and waste products/trace element world averages for brown coals by Ketris and Yudovich [1].

5.2.2. Trace Elements in Bottom Ash and Bottom Ash Size Fractions

Trace element contents in bottom ash and the respective sized fractions are listed in Table 2. Most element contents in bottom ash are enriched compared with those in feed coal. Equal or significantly depleted are some of the volatile elements including Sn, Mo, Sb, F, Bi, Cd, Ge, and Pb. The fractionation of the elements in size is assessed by the enrichment

coefficient (EC), namely the element content in fraction <0.25 mm/element content in fraction >1 mm (Table 2). According to the type of distribution, the elements in the bottom ash size fractions may be grouped as follows:

First group. The contents of Ba, Y, Pr, Sm, Gd, Tb, Dy, Ho, Er, Tm, Yb, Lu, Zr, Hf, Nb, Co, and U increase as the fraction size decreases. Their enrichment coefficient range is 1.2–2.3 (Table 2 and Figure 4A). These concentrations are related to the redistribution of the fuel during the combustion process and the higher presence of unaltered clay minerals, feldspars, and plagioclases in this waste product [27]. Another explanation is the occurrence of these mostly lithophile elements as proper accessory species.

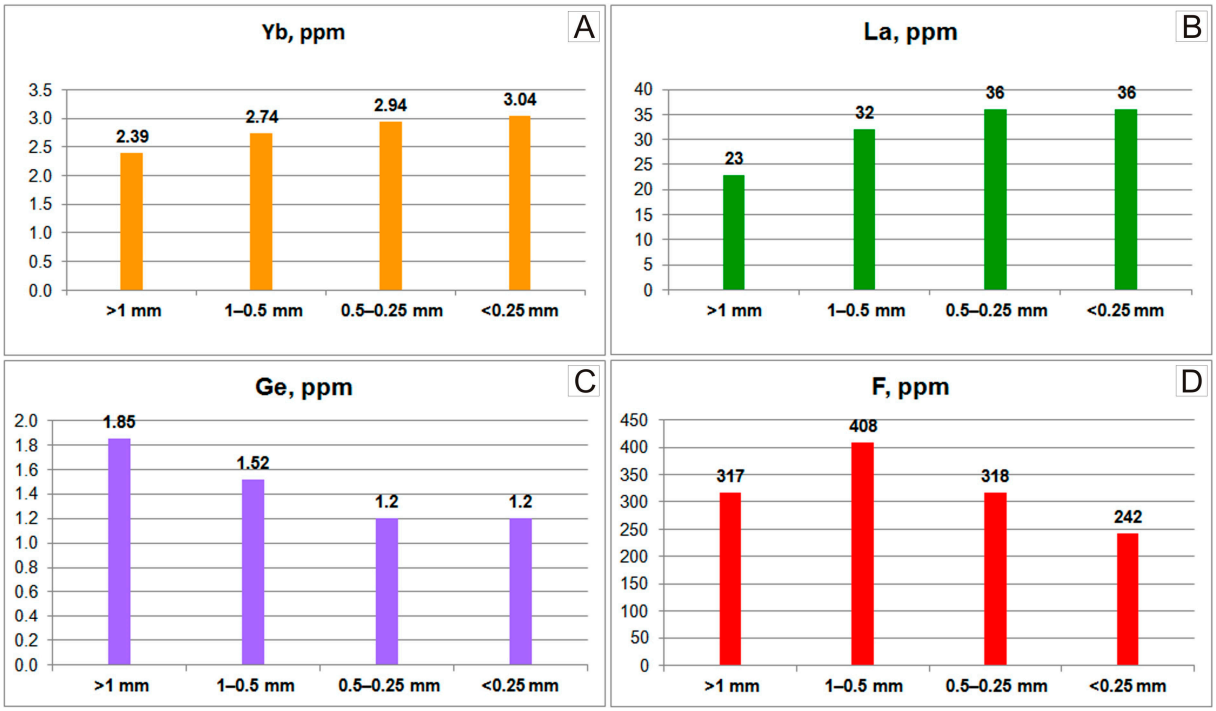

Figure 4. Distribution of the elements in the bottom ash size fractions. (**A**) The first group is represented via Yb. (**B**) The second group is represented via La. (**C**) The third group is represented via Ge. (**D**) The fourth group is represented via F.

Second group. The contents of Li, Rb, Cs, Sr, Tl, Be, Sc, La, Ce, Nd, Eu, Ga, Ta, W, and Th increase up to the 0.5–0.25 mm fraction, and then remain the same or are slightly depleted in the smallest fraction (Figure 4B). These predominantly lithophile elements are probably mainly associated with specific silicates in bottom ash. The contents of Eu can be considered less affected by the occurrence of $^{137}Ba^{16}O$ and $^{136}Ba^{16}OH$ during analysis using quadrupole ICP-MS because the Ba/Eu is much lower than 1000 [4].

Third group. Germanium and Cd are the only elements with decreasing contents towards a fraction <0.25 mm (Figure 4C). Both elements probably have some organic affinity because the ash yield value is the minimum in the coarsest fraction.

Fourth group. Fluorine, V, and most of the sulfophile and siderophile elements (Mo, Sn, Cu, Zn, In, Pb, Sb, Cr, Mn, and Ni) show uneven partitioning with maximum contents in the fraction 1–0.5 mm (Figure 4D). Such complicated segregation may be attributed to combined factors such as the volatility of the elements and the presence of mineral and char particles containing them in this fraction.

On the whole, there is no significant redistribution of the trace elements among the bottom ash size fractions. This may be explained by the similar matrix of the fractions because they contain from 79% to 85% silicates, determined by Vassilev et al. [27], for the bottom ashes of the same boiler. For this reason, the trace element enrichment in the finest fraction (<0.25 mm) is most probably a result of more intensive adsorption processes.

5.2.3. Contents and Distribution of Trace Elements in Fly Ashes

The increased trace element contents in fly ashes produced in many coal-fired power plants are commonly due to the element condensation on the particle surface because the ratio of particle surface/volume is higher in the smallest particles [34,48,53–55]. Another explanation is the occurrence of these mostly lithophile elements in the finest minerals even as proper accessory species.

The trace element contents in the fly ashes from the mechanical collector and two electrostatic precipitator (ESP) rows are listed in Table 3. In order to evaluate the element redistribution, the following enrichment coefficients were calculated: m/b, e1/b, and e2/b, which represent the element contents in the mechanical collector and the 1st and 2nd ESP rows/element contents in the bottom ash, respectively (Table 3). According to these coefficients, the following trends could be distinguished:

From the mechanical collector to the second electrostatic precipitator, the enrichment coefficients of Tl, Be, Ga, Ge, Zr, Hf, Tb, Sn, V, Nb, F, Zn, Cd, In, Pb, Bi, and Sb increase from 1.23 (Be and Hf) to 7.43 (Bi) as can be seen in Table 3. Similar pattern of enrichment have Li, Tb, Dy, Ho, Er, Yb, Lu, Ta, Cu, Cr, Co, and Ni; however, the enrichment coefficient is lower, from 1.05 (Ni) to 1.19 (Ta). The contents of Cs, Y, La, Ce, Pr, Nd, Sm, Gd, Mn, and Th decrease towards the second ESP row. Elements Rb, Sr, Ba, Sc, Tm, Br, and U show uneven partitioning. Chlorine is also unevenly partitioned, with the highest content in the mechanical collector, suggesting its emission with the vapor phases and condensation in this fly ash. Europium is the only element with similar contents and enrichment coefficients in all fly ashes.

Higher contents of trace elements in electrostatic precipitator ashes than in mechanically collected ash were also established for Kentucky power plants [54]. Increasing contents of semi-volatile elements of fly ash with increasing distance from the boiler were found for other coal power plants [55–58].

From the mechanical collector to the ESP, the temperature of the flue gases decreases, which favors the condensation of the elements, depending on their dew point temperature. Another factor favoring element condensation is the greater adsorption/absorption capacity of the smallest particles. The dependence of trace element contents on particle size was earlier established by Davidson et al. [59] and was later confirmed for other power plants [60,61]. However, the exact enrichment mechanism of trace elements of the small particles needs further study [62,63]. Actually, later comparative experiments of trace element concentration on the condensation film of fly ash particles showed that the condensation processes are more complicated and depend as well on the boiling temperature of the elements [64]. For example, the microscopic study of microspheres attached to the surfaces of larger fly ash spheres showed that the former particles have completely different compositions in comparison with the host spheres [65]. It could be suggested that such differences also influence the accumulation of trace elements on fly ash particles. For instance, investigations on the adsorption of Hg on fly ashes reveal that "char has a leading role for the partial capture and retention behavior of Hg in fly ashes" [66]. Moreover, there are differences between the capture mechanism for the fly ashes from the lignite and bituminous coals studied [66]. Hence, in order to elucidate the retention mechanism of elements on fly ashes, further detailed investigations are needed.

According to Meij [56], high volatile elements such as F, Cl, and Br are almost not condensed on fly ash. However, fluorine is highly enriched in the ash of the two ESPs and evenly distributed in the bottom ash size fractions in the Republika TPS. The quantity of fluorine condensed on fly ash depends strongly on the CaO content because CaO can combine F as CaF_2 [67]. Significant F contents were detected in the wastes of a Russian TPS burning brown coals [68]. Additionally, in the fly ash derived from Ge-rich Wulantuga coals (northern China), F content was up to 15568 ppm on an ash basis and the major carrier of F was fluorite [69].

The main conclusion is that during combustion in the Republika TPS, no significant segregation of the trace elements occurs between the bottom ashes and fly ashes, excluding the high volatile and sulfophile elements.

In general, during the process of coal combustion, a great proportion of the trace element contents in the feed coal remains in the solid combustion residues. Such behavior is characteristic of other coal-fired power plants. For instance, similar behavior was observed for ten Turkish power plants [70] and a large Spanish power plant using sub-bituminous coal [71]. The same was established for many Russian power plants where about 82% of the trace elements present in clay minerals (included in the mineral structure or adsorbed) remain in bottom ashes and fly ashes [72].

5.2.4. Behavior of REE

The behavior of the REEs in all samples studied is coherent. Overall, the REE chondrite and shale-normalized patterns are very similar (Figure 5A,B). However, some differences could be pointed out:

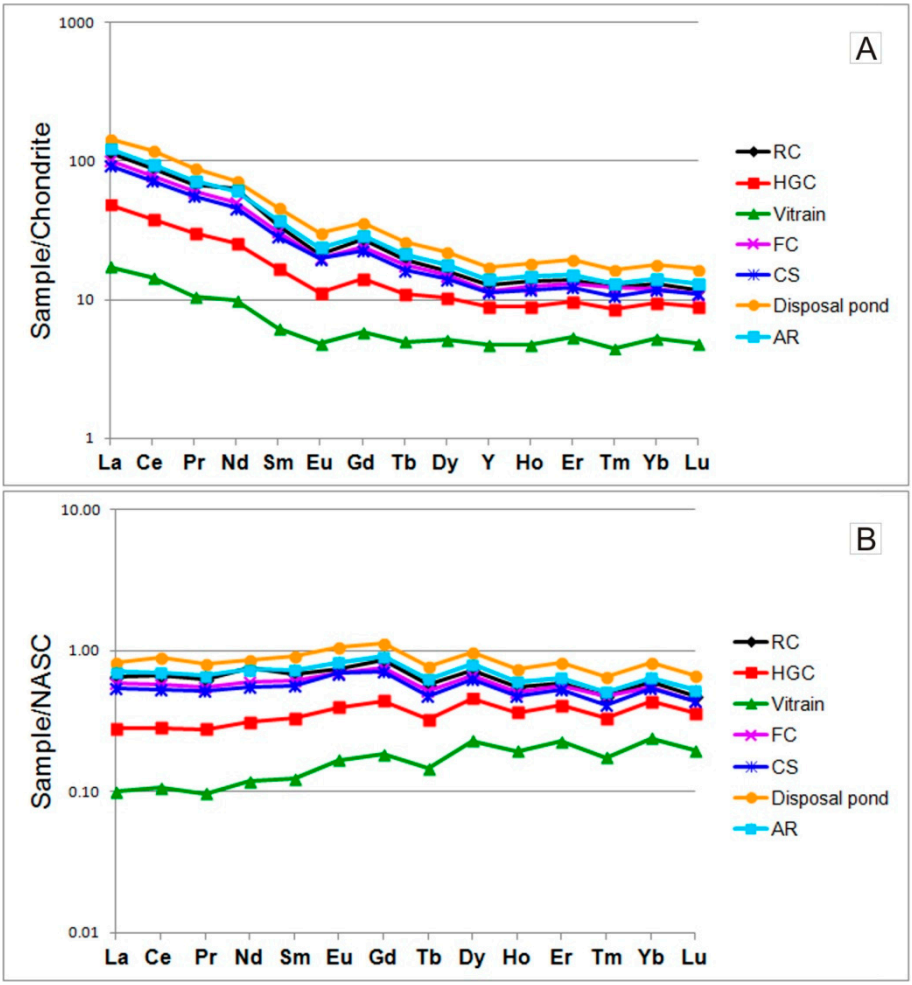

Figure 5. Normalized REE patterns of the Pernik coals and waste products to (**A**) chondrite [33] and (**B**) shales [73].

It can be seen that the ΣREE contents vary significantly (Table 4). The vitrain sample and the high-grade coals have the lowest ΣREE concentrations. Bottom ash and fly ash are enriched in REE compared with feed coal. The ratios LREE (La–Eu)/HREE (Gd–Lu) and Ce_N/Yb_N are lower for vitrain and HGC, indicating a relative HREE enrichment in comparison with the rest of the studied samples. Such enrichment is characteristic of many worldwide coals [74–77] and indicates a stronger organic association of the HREE than

the LREE. It may be presumed that besides the dominant proportion of aluminosilicate-associated REE in the Pernik coals, a small quantity of REE seems to be organically bound.

Table 4. Rare earth elements in coals and combustion wastes.

Samples	RC	HGC	FC	CS	DP	AR	Vitrain	BA	MC	ESP Ash
∑REE	139	51	123	111	290	146	24.4	270	197	192
LREE/HREE	7.8	5.4	6.2	7.2	7.4	7.5	4.09	7.58	7.58	7.32
Ce_N/Yb_N [1]	6.87	4.05	6.53	6.11	6.71	6.71	2.77	6.71	6.76	6.95
Eu/Eu* [1]	0.69	0.72	0.72	0.77	0.74	0.72	0.79	0.75	0.72	0.72

MC—mechanical collector ash; [1]—chondrite-normalized values.

During the combustion process, a slight differentiation occurs between the light and heavy REEs. In the fractions of bottom ash, the mean e/d coefficient for the LREEs is 1.5, while for the HREEs it is 1.3, suggesting higher adsorption/condensation on the smaller fractions (Table 4). These differences are also distinctive for the fly ash from the mechanical collector. For example, the LREE contents slightly decrease, while HREE concentrations slightly increase for fly ashes from the mechanical collector to the second ESP row. These differences may be attributed to organically associated REEs, whose mobility (particularly of the HREEs) is higher than that of aluminosilicate-associated REEs. Differences in the mobility between light and heavy REEs have been experimentally established for some Chinese and Spanish coals and their combustion wastes [69,78,79].

It was also found that the europium anomaly (Eu/Eu* = 0.69–0.79) in chondrite-normalized patterns is very weak for all samples studied (Table 4 and Figure 5) and non-existent in NASC-normalized patterns (Eu/Eu* = 0.98–1.1). This observation is quite different compared with that for high-Ge coals and their combustion products from some Chinese TPSs [69].

In summary, the REEs are rather evenly distributed in the different combustion products attributed to their predominant aluminosilicate association. The REY contents of the studied samples are plotted in the unpromising area field (Figure 6) in the diagram of Dai et al. [80].

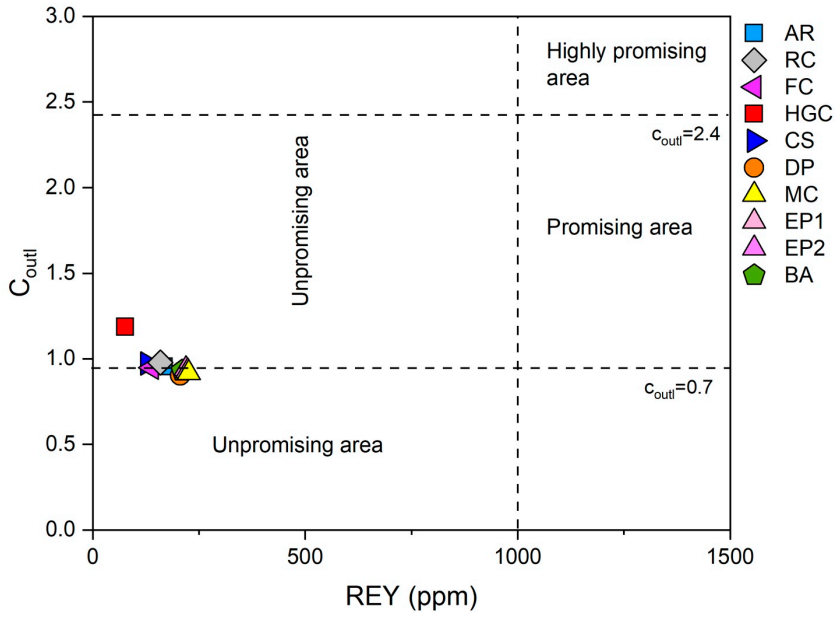

Figure 6. Evaluation of REY in the studied samples using the outlook coefficient (Coutl), established by Seredin and Dai [2], in a plot as in Dai et al. [80].

5.2.5. Correlations

Correlation coefficients (r) between the mean element contents of the raw coal, high-grade coal, feed coal, coal slurry, wastes from disposal pond, and associated rocks (Table 1) were calculated in order to distinguish some trends in their distribution and associations. For the six types of samples, the statistically significant correlation coefficients are $\geq$0.70 at a 95% confidence level. Most elements have a positive correlation ($r \geq 0.70$) with ash yield, indicating their inorganic association. The correlation of F (r = 0.68), Sr (r = 0.64), Cs (r = 0.63), and Ge (r = 0.62) with ash yield is also positive, but insignificant.

The remaining elements are characterized by the corresponding correlation coefficients with ash yield: Be (r = 0.53), Bi (r = 0.45), Cd (r = 0.26), Br (r = −78), S (r = −0.85), and Mo (r = −0.72). Beryllium correlates positively and significantly ($r \geq 0.70$) with Y, HREEs, V, W, Cl, Co, and Ni; bismuth correlates positively and significantly ($r \geq 0.70$) with F, Sr, Br, Cs, Sn, and Nd; cadmium correlates positively and significantly (r = 0.78) with Pb; bromine correlates positively and significantly with Bi (r = 0.84) and F (r = 0.74); and molybdenum is positively and insignificantly correlated to Cl (r = 0.43). This group of elements correlates with those that have an affinity to the organic matter (vitrain, clarain, and fusain), present as property phases, or are volatile.

Elements can have a mixed mode of occurrence, but their behavior depends on the dominant one. For example, Mo has been found as an impurity in pyrite [27], but it has the highest concentrations in the samples with low ash yield as vitrine and HGC. This implies allowing for its affinity to organic matter and the autogenous mineralization that is intimately related to it (Figure 2A).

The correlations between the trace elements confirm their behavior outlined above as follows: limited partitioning among the combustion products for most elements and low, or lack of correlation to ash or volatile elements.

6. Environmental Aspects

As stated by Swaine [38], "with the modern facilities, there is a reduction in the amounts of trace elements in stack emissions relative to those in bottom and fly ash". Hence, more attention must be given to the fate of trace elements in coal wastes, in particular to losses caused by leaching to nearby waters. The wastes from the Pernik preparation coal plant and Republika power station (coal slurry, bottom, and fly ashes) are transported to a disposal pond by water.

The wastes are enriched or depleted in different trace elements compared with that in feed coal. For example, the trace elements in the slurry are slightly depleted with the exclusion of Cl (3.8×), Ba (1.7×), and Br (1.3×). Most elements in bottom ash are about 1.5× higher, while some volatile elements are of equal or lower contents (Ge, Sn, Mo, Sb, Cd, Pb, and F). Fly ash is enriched (1.4×–1.8×) in all elements with the exception of the highly volatile Br only.

Compared with the feed coals, the whole mix in the disposal pond is strongly concentrated in Cl (4.3×), as the element was introduced with the water transporting the waste products (Table 1). The enrichment of most elements ranges from 1.23 to 1.75. Only some volatile elements are depleted—Ge, Mo, Br, F, and Bi, suggesting their release with the flue gases.

As the enrichment of trace elements in bottom ash and especially in fly ash particles is the result of some sorption processes on their surface, the elements are subjected to possible leaching and migration. Hence, this topic is very important from an environmental point of view and requires additional investigations.

On the other hand, the coal slurry is also a source of some mobile elements such as F, V, As, Pb, Mo, Li, Sr, Ti, Ga, Ni, Ge, Cr, and Mn (Table 1), and according to Yossifova, 2007 [27]. These elements can migrate from the sludge into the water of the disposal pond. The mobility of such elements strongly depends on the concentration of their mode of occurrence, for instance, (1) proper phases (halites, sulfates, carbonates, and sulfides);

(2) impurity elements in the above mobile minerals; or (3) sorbed species of mobile elements in organic matter and clay minerals [27,81].

7. Conclusions

The Pernik coals have trace element contents normally higher than the respective Clarke contents for brown coals worldwide and some of these elements may be of environmental concern.

It was found that some trace elements are more enriched (more than two times) in the associated rocks in comparison with coals, namely Cs, Sc, Nd, Sm, Eu, Gd, Tb, Dy, Ho, Sn, F, Cu, Pb, Cr, Co, Th, Li, Tl, La, Ce, Pr, Ta, and Zn. The predominant inorganic association of most trace elements was confirmed by the comparison of their contents with that of a vitrain sample that is depleted in ash yield (8.8%). On the other hand, vitrain is strongly enriched in V and, to a lesser extent, Mo, Ni, Pb, Co, W, F, Nb, and Cu. The dominant inorganic affinity of the trace elements in coal has a leading role in their behavior during combustion because a great part of them is retained in solid waste products. Moreover, it was identified that most trace elements are not significantly redistributed between the different combustion wastes. In contrast, the highly volatile elements (F, Cl, and Br) and volatile elements (Bi, Ge, Zn, Sb, Cd, Mo, Sn, and Tl) are significantly partitioned between the fly ashes from the mechanical collector and the ESP. The hazardous trace elements appear to be mainly retained in the waste products and there are no appreciable emissions of them into the atmosphere with the flue gases. However, the organically bound trace elements tend to appear as vapor phases in the boiler during combustion.

Author Contributions: G.M.E. wrote the geochemical part of the manuscript. M.G.Y. wrote the mineralogical part of the manuscript. D.A.D. prepared the graphical visualization of the results. S.V.V. reviewed and revised the text in English. All authors have read and agreed to the published version of the manuscript.

Funding: The trace element analysis was financially supported by the National Key Basic Research program of China (No.2014CB238902).

Data Availability Statement: All data of this research is presented within the manuscript.

Acknowledgments: The authors are grateful to S. Dai, P. Wang, and X. Li for conducting the chemical analyses. The authors appreciate the remarks of the reviewers which helped to improve the manuscript.

Conflicts of Interest: The authors declare no conflicts of interest.

References

1. Ketris, M.P.; Yudovich, Y.E. Estimation of Clarkes for Carbonaceous biolithes: World averages for trace element contents in black shales and coals. *Int. J. Coal Geol.* **2009**, *78*, 135–148. [CrossRef]
2. Seredin, V.V.; Dai, S. Coal deposits as potential alternative sources for lanthanides and yttrium. *Int. J. Coal Geol.* **2012**, *94*, 67–93. [CrossRef]
3. Dai, S.; Liu, J.; Ward, C.R.; Hower, J.C.; French, D.; Jia, S.; Hood, M.M.; Garrison, T.M. Mineralogical and geochemical compositions of Late Permian coals and host rocks from the Guxu Coalfield, Sichuan Province, China, with emphasis on enrichment of rare metals. *Int. J. Coal Geol.* **2015**, *166*, 71–95. [CrossRef]
4. Dai, S.; Graham, I.T.; Ward, C.R. A review of anomalous rare earth elements and yttrium in coal. *Int. J. Coal Geol.* **2016**, *159*, 82–95. [CrossRef]
5. Dai, S.; Hower, J.C.; Finkelman, R.B.; Graham, I.T.; French, D.; Ward, C.R.; Eskenazy, G.; Wei, Q.; Lei Zhao, L. Organic associations of non-mineral elements in coal: A review. *Int. J. Coal Geol.* **2020**, *218*, 103347. [CrossRef]
6. Arbuzov, S.I.; Chekryzhov, I.Y.; Spears, D.A.; Ilenok, S.S.; Soktoev, B.R.; Popov, N.Y. Geology, geochemistry, mineralogy and genesis of the Spetsugli high-germanium coal deposit in the Pavlovsk coalfield, Russian Far East. *Ore Geol. Rev.* **2021**, *139*, 104537. [CrossRef]
7. Dai, S.; Arbuzov, S.I.; Chekryzhov, I.Y.; French, D.; Feole, I.; Folkedahl, B.C.; Graham, I.T.; Hower, J.C.; Nechaev, V.P.; Wagner, N.J.; et al. Metalliferous Coals of Cretaceous Age: A Review. *Minerals* **2022**, *12*, 1154. [CrossRef]
8. Liu, T.; Hower, J.C.; Huang, C.-H. Recovery of Rare Earth Elements from Coal Fly Ash with Betainium Bis(trifluoromethylsulfonyl) imide: Different Ash Types and Broad Elemental Survey. *Minerals* **2023**, *13*, 952. [CrossRef]

9. Santos, A.C.; Cruz, C.; Font, E.; French, D.; Guedes, A.; Moreira, K.; Sant'Ovaia, H.; Vieira, B.J.C.; Waerenborgh, J.C.; Valentim, B. Physicochemical Properties of Fe-Bearing Phases from Commercial Colombian Coal Ash. *Minerals* **2023**, *13*, 1055. [CrossRef]
10. Wang, X.; Feng, Q.; Sun, R.; Liu, G. Radioactivity of Natural Nuclides (^{40}K, ^{238}U, ^{232}Th, ^{226}Ra) in Coals from Eastern Yunnan, China. *Minerals* **2015**, *5*, 637–646. [CrossRef]
11. Jia, J.; Li, X.; Wu, P.; Liu, Y.; Han, C.; Zhou, L.; Yang, L. Human Health Risk Assessment and Safety Threshold of Harmful Trace Elements in the Soil Environment of the Wulantuga Open-Cast Coal Mine. *Minerals* **2015**, *5*, 837–848. [CrossRef]
12. Gerson, A.R.; Fan, R.; Qian, G.; Schumann, R.C.; Olin, P.; Howard, D.L.; Smart, R.S.C. Examination of multiple sources of selenium release from coal wastes and strategies for remediation. *J. Hazard. Mater.* **2022**, *422*, 126924. [CrossRef]
13. Yang, J.; Tu, C.; Jiang, Q.; Wang, J.; Li, L.; Finkelman, R.B. Analysis of multiple pathways and levels of fluoride intake in fluorosis areas of Southwest China. *Heliyon* **2023**, *9*, e13651. [CrossRef]
14. Finkelman, R.B.; Dodds, H.R.; Naomi, T.; Nichols, N.T.; Stracher, G.B. Coal Fire Sublimates: Are We Missing Something? *Sustainability* **2023**, *15*, 16262. [CrossRef]
15. Stanislav, V.; Vassilev, S.V.; Vassileva, C. A retrospection on the content, association, and significance of mercury in coals and coal ashes from Bulgarian thermoelectric power stations. *J. Hazard. Mater.* **2023**, *457*, 131850. [CrossRef]
16. Yudovich, Y.E.; Ketris, M.P. *Inorganic Matter of Coal*; Russian Academia of Science Ural Division: Ekaterinburg, Russia, 2002; 421p. (In Russian)
17. Yudovich, Y.E.; Ketris, M.P. *Toxic Trace Elements in Coal*; Russian Academie of Science Ural Division: Ekaterinburg, Russia, 2005; 634p. (In Russian)
18. Yudovich, Y.E.; Ketris, M.P. *Valuable Trace Elements in Coal*; Russian Academie of Science Ural Division: Ekaterinburg, Russia, 2006; 538p. (In Russian)
19. Dai, S.; Finkelman, R.B.; Hower, J.C.; French, D.; Graham, I.T.; Zhao, L. *Inorganic Geochemistry of Coal*; Elsevier: Amsterdam, The Netherlands, 2023; 300p.
20. Greta, E.; Dai, S.; Li, X. Fluorine in Bulgarian coals. *Int. J. Coal Geol.* **2013**, *105*, 16–23. [CrossRef]
21. The European Commission. *Study on the Critical Raw Materials for the EU 2023—Final Report*; EU Publications: Luxembourg, 2023.
22. Koniarov, G. *The Brown Coals in Bulgaria*; Issue of the Government Pernik Mines: Pernik, Bulgaria, 1932; 303p. (In Bulgarian)
23. Silva, L.F.O.; Da Boit, K.; Sampaio, C.H.; Jasper, A.; Andrade, M.L.; Kostova, I.J.; Waanders, B.; Henke, K.R.; Hower, J.C. The occurrence of hazardous volatile elements and nanoparticles in Bulgarian coal fly ashes and the effect on human health exposure. *Sci. Total Environ.* **2012**, *416*, 513–526. [CrossRef]
24. Vassilev, S.V.; Vassileva, C.G. Mineralogy of combustion wastes from coal-fired power stations. *Fuel Process. Technol.* **1996**, *47*, 261–289. [CrossRef]
25. Vassilev, S.V.; Vassileva, C.G. Geochemistry of coals, coal ashes and combustion wastes from coal-fired power stations. *Fuel Process. Technol.* **1997**, *51*, 19–45. [CrossRef]
26. Vassilev, S.; Eskenazy, G.; Karaivanova, E. Chlorine and bromine in Bulgarian coals and their combustion products. *C. R. Acad. Bulg. Sci.* **1997**, *50*, 7–8.
27. Vassilev, S.; Eskenazy, G.; Vassileva, C. Behaviour of elements and minerals during preparation and combustion of the Pernik coal, Bulgaria. *Fuel Process. Technol.* **2001**, *72*, 103–129. [CrossRef]
28. Yossifova, M. Mineral and inorganic chemical composition of the Pernik coal, Bulgaria. *Int. J. Coal Geol.* **2007**, *72*, 268–292. [CrossRef]
29. *ISO 1171:2010*; Solid Mineral Fuels—Determination of Ash. Fourth Edition. International Organization for Standardizatio: Geneva, Switzerland, 2010.
30. Dai, S.; Wang, X.; Zhou, Y.; Hower, J.C.; Li, D.; Chen, W.; Zhu, X.; Zou, J. Chemical and mineralogical compositions of silicic, mafic, and alkali tonsteins in the late Permian coals from the Songzao Coalfield, Chongqing, Southwest China. *Chem. Geol.* **2011**, *282*, 29–44. [CrossRef]
31. *ASTM Standard D5987-96*; Standard Test Method for Total Fluorine in Coal and Coke by Pyrohydrolytic Extraction and Ion Selective Electrode or Ion Chromatograph Methods. ASTM International: West Conshohocken, PA, USA, 2002; Reapproved 2007.
32. Dai, S.; Seredin, V.; Ward, C.R.; Hower, J.C.; Xing, Y.; Zhang, W.; Song, W.; Wang, P. Enrichment of U–Se–Mo–Re–V in coals preserved within marine carbonate successions: Geochemical and mineralogical data from the Late Permian Guiding Coalfield, Guizhou, China. *Miner. Depos.* **2015**, *50*, 159–186. [CrossRef]
33. MacDonough, W.; Sun, S. The composition of the Earth. *Chem. Geol.* **1995**, *120*, 223–253. [CrossRef]
34. Dai, S.; Zhao, L.; Peng, S.; Chou, C.L.; Wang, X.; Zhang, Y.; Li, D.; Sun, Y. Abundances and distribution of minerals and elements in high-alumina coal fly ash from the Jungar Power Plant, Inner Mongolia, China. *Int. J. Coal Geol.* **2010**, *81*, 320–332. [CrossRef]
35. Finkelman, R.B. The use of modes of occurrence information to predict the removal of the hazardous air pollutants prior to combustion. *J. Coal Qual.* **1993**, *12*, 132–134.
36. Kler, V.; Nenahova, V. *Paragenetic Complexes of Shale- and Coal-Bearing Seams*; Nauka: Moscow, Russia, 1981; 175p. (In Russian)
37. Shpirt, M. *Technology without Wastes. Utilization of Wastes from Mining and Preparation of Coal*; Nedra: Moskow, Russia, 1986; 254p. (In Russian)
38. Swaine, D.J. Trace elements during the mining and beneficiation of coal. *Coal Prep.* **1998**, *19*, 177–193. [CrossRef]
39. Vassilev, S. Phase mineralogy studies of solid waste products from coal burning at some Bulgarian thermoelectric power plants. *Fuel* **1992**, *71*, 625–633. [CrossRef]

40. Yossifova, M.; Valćeva, S.; Djourova, E. Mineralogy and environmental geochemistry of lagooned ashes resulted from combustion of Maritza East lignite, Bulgaria. *Int. J. Coal Geol.* **2007**, *71*, 287–302. [CrossRef]
41. Hower, J.C. Petrographic examination of coal-combustion fly ash. *Int. J. Coal Geol.* **2012**, *92*, 90–97. [CrossRef]
42. Varma, A.K.; Kumar, M.; Saxena, V.K.; Sarkar, A.; Banerjee, S.K. Petrographic controls on combustion behavior of inertinite rich coal and char and fly ash formation. *Fuel* **2014**, *128*, 199–209. [CrossRef]
43. Hower, J.C.; Groppo, J.G.; Graham, U.M.; Ward, C.R.; Kostova, I.J.; Maroto-Valer, M.M.; Dai, S. Coal-derived unburned carbons in fly ash: A review. *Int. J. Coal Geol.* **2017**, *179*, 11–27. [CrossRef]
44. Yossifova, M.; Valčeva, S. Preliminary data on the phase-mineral composition of burned coals and host rocks during spontaneous combustion in Pernik and Berovo coal basins. In *Anniversary Proceedings "60 Years of Geological Course", Sofia University "St. Kliment Ohridski"*; Sofia University: Sofia, Bulgaria, 2008; pp. 75–80.
45. Amalia Jiménez, A.; Jose´ Iglesias, M.J.M.; Laggoun-Defarge, F.; Isabel Suárez-Ruiz, I. Effect of the increase in temperature on the evolution of the physical and chemical structure of vitrinite. *J. Anal. Appl. Pyrolysis* **1999**, *50*, 117–148. [CrossRef]
46. Wang, Y.; Lian, J.; Xue, Y.; Liu, P.; Dai, B.; Lin, H.; Han, S. The pyrolysis of vitrinite and inertinite by a combination of quantum chemistry calculation and thermogravimetry-mass spectrometry. *Fuel* **2020**, *264*, 116794. [CrossRef]
47. Guedes, A.; Valentin, B.; Prieto, A.C.; Sanz, A.; Flores, D.; Noronha, F. Characterization of fly ash from a power plant and surroundings by micro-Raman spectroscopy. *Int. J. Coal Geol.* **2008**, *73*, 359–370. [CrossRef]
48. Mardon, S.M.; Hower, J.S.; O'Keefe, J.M.K.; Marks, M.N.; Hedges, D.H. Coal combustion by-product quality at two stoker boilers: Coal source vs. fly ash collection system design. *Int. J. Coal Geol.* **2008**, *75*, 248–254. [CrossRef]
49. Huggins, F.; Goodarzi, F. Environmental assessment of elements and polyaromatic hydrocarbons emitted from a Canadian coal-fired power plant. *Int. J. Coal Geol.* **2009**, *77*, 282–288. [CrossRef]
50. Atanasova-Vladimirova, S. Petrology of the Vitosha Pluton. Ph.D. Thesis, Geological Institute, Bulgarian Academy of Sciences, Sofia, Bulgaria, 2015; 160p. (In Russian).
51. Christova, J.; Christov, D.; Kuikin, S. Background contents of some minor and trace elements in the rocks on Bulgarian territory. *Geol. Balc.* **2007**, *36*, 65–76. [CrossRef]
52. Hikov, A. Geochemistry of hydrothermally altered rocks in Klisoura occurrence, Sofia District. *Geol. Balc.* **2002**, *32*, 89–92. [CrossRef]
53. Kunov, A.; Stamatova, V.; Atanassova, R.; Christova, V.; Stanchev, C. New data of wallrock alteration and ore mineralizations from the Klisoura occurrence, Sofia district. *Rev. Bulg. Geol. Soc.* **2000**, *61*, 143–150.
54. Hower, J.C.; Robertson, J.D.; Thomas, G.A.; Wong, A.S.; Schram, W.H.; Graham, U.M.; Rathbone, R.F.; Robl, T.I. Characterization of fly ash from Kentucky power plants. *Fuel* **1996**, *75*, 402–411. [CrossRef]
55. Hower, J.C.; Trimble, A.S.; Eble, C.F.; Palmer, C.A.; Kolker, A. Characterization of fly ash from low-sulfur and high-sulfur coal sources: Partitioning of carbon and trace elements with particle size. *Energy Sources* **1999**, *25*, 511–525.
56. Meij, R. The distribution of trace elements during the combustion of coal. In *Environmental Aspects of Trace Elements in Coal*; Swaine, D.J., Goodarzi, F., Eds.; Kluwer Academic Publishers: Norwell, MA, USA, 1995; pp. 111–127.
57. Mardon, S.M.; Hower, J.C. Impact of coal properties on coal combustion by-product quality: Examples from a Kentucky power plant. *Int. J. Coal Geol.* **2004**, *59*, 153–169. [CrossRef]
58. Mastalerz, M.; Hower, J.C.; Drobniaka, A.; Mardon, S.M.; Lis, G. From in-situ coal to fly ash: A study of coal mines and power plants from Indiana. *Int. J. Coal Geol.* **2004**, *59*, 171–192. [CrossRef]
59. Davidson, R.L.; Natusch, D.F.C.; Wallace, J.R.; Evans, C.A. Trace elements in fly ash–dependence of concentration on particle size. *Environ. Sci. Technol.* **1974**, *8*, 1107–1113. [CrossRef]
60. Smith, R.D. The trace element chemistry of coal during combustion and the emissions from coal-fired power plants. *Prog. Energy Combust. Sci.* **1980**, *6*, 53–119. [CrossRef]
61. Querol, X.; Fernandez-Turiel, I.L.; Copez-Soler, A. Trace elements in coal and their behavior during combustion in a large power station. *Fuel* **1995**, *74*, 331–343. [CrossRef]
62. Hulett, L.D.; Weinberger, A.J. Some etching studies of the microstructure and composition of large aluminosilicate particles in fly ash from coal-burning power plants. *Environ. Sci. Technol.* **1980**, *14*, 965–970. [CrossRef] [PubMed]
63. Smith, R.D.; Baer, D.R. Fly ash surface formation and segregation during heating. *Atmos. Environ.* **1983**, *17*, 1399–1409. [CrossRef]
64. Kisilstein, L.Y. Concentration of trace elements on the fly ash surfaces from coal-fired thermoelectric power plants. *Solid Fuel Chem.* **1993**, *6*, 91–96. (In Russian)
65. Booher, H.; Martello, D.; Tamilia, J.; Irdi, G. Microscopic study of spheres and microspheres in fly ash. *Fuel* **1994**, *73*, 205–213. [CrossRef]
66. Kostova, I.; Vassileva, C.; Dai, S.; Hower, J.C.; Apostolova, D. Influence of surface area properties on mercury capture behavior of coal fly ashes from some Bulgarian power plants. *Int. J. Coal Geol.* **2013**, *116–117*, 227–235. [CrossRef]
67. Yudovich, Y.; Ketris, M. Fluorine in coal: A review. *Biosphere* **2010**, *2*, 59–72. (In Russian)
68. Boiko, S.M.; Suturin, A.N. Geochemistry of the commercial coal ash from the Asei deposit and problems of its utilization. *Russ. Geol. Geophys.* **1994**, *35*, 100–108.
69. Dai, S.; Seredin, V.V.; Ward, C.R.; Jiang, J.; Hower, J.C.; Song, X.; Jiang, Y.; Wang, X.; Gornostaeva, T.; Li, X.; et al. Composition and mode of occurrence of minerals and elements in coal combustion products derived from high-Ge coals. *Int. J. Coal Geol.* **2014**, *121*, 79–97. [CrossRef]

70. Gayer, R.A.; Karayigit, A.I.; Goldsmith, S.; Onacak, T.; Rose, M. Trace element geochemistry of feed coals, fly and bottom ashes of Turkish power plants: Implications for ash utilization. In Proceedings of the AIE 8th Australian Coal Science Conference, Sydney, Australia, 7–9 December 1998; pp. 339–344.
71. Llorens, J.F.; Fernandez-Turiel, J.L.; Querol, X. The fate of trace elements in a large coal-fired power plant. *Environ. Geol.* **2001**, *40*, 409–416. [CrossRef]
72. Kisilstein, L.Y.; Levchenko, S.V.; Peretyatko, A.G. Formation of the trace elements gaseous phase during coal combustion in power plants. *Solid Fuel Chem.* **1990**, *6*, 136–139. (In Russian)
73. Piper, D.Z. Rare earth elements in the sedimentary cycle: A summary. *Chem. Geol.* **1974**, *14*, 285–298. [CrossRef]
74. Ershov, V.M. Rare earth elements in the Kiselovsk Basin, Russia. *Geochimia* **1961**, *3*, 274–276. (In Russian)
75. Eskenazy, G.M. Rare earth elements and yttrium in lithotypes of Bulgarian coals. *Org. Geochem.* **1987**, *11*, 83–89. [CrossRef]
76. Eskenazy, G.M. Rare earth elements in a sampled coal from the Pirin Deposit, Bulgaria. *Int. J. Coal Geol.* **1987**, *7*, 301–314. [CrossRef]
77. Dai, S.; Zhang, W.; Ward, C.R.; Seredin, V.V.; Hower, J.C.; Li, X.; Song, W.; Kang, H.; Zheng, L.; Zhou, D. Mineralogical and geochemical anomalies of Late Permian coals from the Fusui Coalfield, Guangxi Province, Southern China: Influences of terrigenous materials and hydrothermal fluids. *Int. J. Coal Geol.* **2013**, *105*, 60–84. [CrossRef]
78. Querol, X.; Juan, R.; Lopez-Soler, A.; Fernandez-Turiel, J.L.; Ruiz, C.R. Mobility of trace elements from coal and combustion wastes. *Fuel* **1996**, *75*, 821–838. [CrossRef]
79. Dai, S.; Zhao, L.; Hower, J.C.; Jonston, M.N.; Song, W.; Wang, P.; Zhang, S. Petrology, mineralogy, and chemistry of size fractions fly ash from the Jungar Power Plant, Inner Mongolia, China, with emphasis on the distribution of REE. *Energy Fuels* **2014**, *28*, 1502–1514. [CrossRef]
80. Dai, S.; Xie, P.; Ward, C.R.; Yan, X.; Guo, W.; French, D.; Graham, I.T. Anomalies of rare metals in Lopingian super-high-organic-sulfur coals from the Yishan Coalfield, Guangxi, China. *Ore Geol. Rev.* **2017**, *88*, 235–250. [CrossRef]
81. Yossifova, M. Environmental aspects related to the impact of waste water from coal dressing on human health. *Geol. Miner. Resour.* **2000**, *3*, 25–28.